

Article

Columnar Structure of Claw Denticles in the Coconut Crab, *Birgus latro*

Tadanobu Inoue ^{1,*} , Shin-ichiro Oka ², Koji Nakazato ¹ and Toru Hara ¹ 

¹ National Institute for Materials Science, 1-2-1, Sengen, Tsukuba 305-0047, Japan; nakazato.koji@nims.go.jp (K.N.); hara.toru@nims.go.jp (T.H.)

² Okinawa Churashima Foundation, 888 Ishikawa, Motobu, Okinawa 905-0206, Japan; sh-oka@okichura.jp

* Correspondence: inoue.tadanobu@nims.go.jp; Tel.: +81-29-859-2148; Fax: +81-29-859-2101

Abstract: Some decapod crustaceans have tooth-like white denticles that exist only on the pinching side of claws. We revealed the denticle microstructure in the coconut crab, *Birgus latro*, using optical and scanning electron microscopy (SEM), energy dispersive X-ray spectroscopy (EDS), and a focused ion beam (FIB)-SEM. Three-dimensional analysis and fracture surface observation were performed in order to clarify the microstructural differences in two mineralized layers—the exocuticle and the endocuticle. The denticles consist of a columnar structure normal to the surface and are covered with a very thin epicuticle and an exocuticle with a twisted plywood pattern structure. Due to abrasion, the exocuticle layer was lost in the wide area above the large denticles; conversely, these layers remained on the surface of the relatively small denticles and on the base of the denticle. The results showed that the mineralized exoskeleton of the crab’s claw is classified into three structures: a twisted plywood pattern structure stacked parallel to the surface for the exocuticle, a porous structure with many regularly arranged pores vertical to the surface for the endocuticle, and a columnar structure vertical to the surface for the denticle.



Citation: Inoue, T.; Oka, S.-i.; Nakazato, K.; Hara, T. Columnar Structure of Claw Denticles in the Coconut Crab, *Birgus latro*. *Minerals* **2022**, *12*, 274. <https://doi.org/10.3390/min12020274>

Academic Editors: Linus Stegbauer, Anne Jantschke and Fabio Nudelman

Received: 14 January 2022

Accepted: 16 February 2022

Published: 21 February 2022

Publisher’s Note: MDPI stays neutral with regard to jurisdictional claims in published maps and institutional affiliations.



Copyright: © 2022 by the authors. Licensee MDPI, Basel, Switzerland. This article is an open access article distributed under the terms and conditions of the Creative Commons Attribution (CC BY) license (<https://creativecommons.org/licenses/by/4.0/>).

Keywords: biomineralization; tissue structure; 3-D analysis; fracture surface; crustacean cuticle

1. Introduction

Organisms are designed to respond and adapt well to dynamically changing environments, and they show outstanding mechanical properties. Naturally occurring organisms, like coconut crabs, are not designed, they have been shaped by adaptation as well as phylogenetic and developmental constraints. Biomineralized tissues and structures are a valuable source of design concepts for man-made materials [1,2]. In fact, bio-inspired materials with excellent functional and mechanical properties continue to be reported [3–7].

The exoskeleton that supports and protects the body of all arthropods is mainly composed of four layers: the epicuticle, exocuticle, endocuticle, and membrane [8–10]. Among them, the exocuticle and endocuticle layers comprised of chitin and protein are tough and play an important role in protection from enemies. In crustaceans, these two layers are mineralized and very hard, and these tissues are characterized by a twisted plywood pattern structure [3,11–14]. In the body covered by the exoskeleton, the claws are the most mineralized and have superior mechanical properties as compared to the carapace (cephalothorax), legs, and abdomen [15–17]. The pinching side of the claw displays tooth-like denticles. Waugh et al. [18] reported that the denticles were composed primarily of modified endocuticle, with little or no epi- or exocuticle present in this region in adult crabs. Rosen et al. [19] examined the microstructure, components, and microhardness of the denticles for three brachyuran crabs and two anomuran crabs; they reported that hardness was 2.5 to 10 times higher in the denticle than in the endocuticle, that there was a decrease in the width of the pore canals that run through the cuticle and in the phosphorous content, and that there was a structure change from endocuticle to denticle. Besides, a small

amount of exocuticle (~100 μm thick), characterized by a twisted plywood pattern structure covering the denticle, was visible only in the red king crab, *Paralithodes camtschaticus*. In our previous paper [20], we showed that the calcium concentration in the claw denticles of the coconut crab, *Birgus latro*, was slightly lower than that in the exocuticle, phosphorus concentrations were almost zero, and magnesium concentrations were high as compared to the exocuticle and endocuticle. However, curiously, the maximum hardness (H_{max}) and stiffness ($E_{r(max)}$) near the denticle surface indicated almost the same values, $H_{max} = 4$ GPa and $E_{r(max)} = 70$ GPa. Moreover, a distinct shift in tissue structure from the denticle to the endocuticle in the coconut crab claw has been reported. The tissue mainly aligned normally with the surface within the denticle. This feature was also visible in the claw denticles of brachyuran crabs and anomuran crabs [19]. However, the microstructure of the denticle could not be characterized by scanning electron microscope (SEM), as compared to other cuticle layers. Although the denticles are very important sites that come into direct contact with predators and prey, the microstructure of the denticle has not been clarified. Although the exoskeleton of claw is calcite regardless of each layer of the exocuticle, endocuticle and denticle, as shown in Figure S1 in the supporting information, the denticle microstructure is likely to have a tissue structure that is different from the other mineralized layers. We have clarified that claw denticles in the coconut crab are characterized by a columnar structure through detailed observations of a fracture surface and from the denticle top and three-dimensional analysis by SEM.

2. Materials and Methods

2.1. Sample Preparation

A coconut crab [21] was captured at the town of Motobu on northern Okinawa Island, located in southwestern Japan. The coconut crab was male, and its thoracic length and body weight were 65.7 mm and 1650 g, respectively. This crab was estimated to be an adult 20–26 years old based on the growth model of the southern Japan population [22]. The removed left claw was frozen, transported to National Institute for Materials Science in Tsukuba, and stored at -18 °C prior to analysis. We considered crab welfare and maintained the specimens as described below with the advice of a veterinarian. When removing the claw, the general anesthesia was applied by dipping the claw into cold ice water (approximately 0–4 °C) to avoid pain. The crab was returned to its original area after removing the claw. We also confirmed that some released crabs live normally in wild conditions based on our preliminary study. We have been conducting 15 years of ecological monitoring of wild populations based on individual identification [22,23]. We could find the injured crabs, lacking claws and legs, and confirm their recovery in many cases sometimes. In fact, two of the released crabs in this study have been recaptured in good health after recent monitoring surveys. Based on the above, we believe that the handling of coconut crabs does not have a significant impact on their life or the maintenance of their population and does not conflict with ethical issues. The claw was thawed under running water, and the movable finger was broken by applying a force opposite to the range of motion, and the fixed finger was cut using a saw, as shown in Figure 1a. The denticles are visible on the pinching side of each finger, and the irregularly arranged denticles of various sizes are clearly observed in the cross-sectional image after polishing in Figure 1b. A SEM image of the exoskeleton with a denticle and a high-magnification SEM image of the denticle surface are shown in Figure 1c,d. Details of the procedures and microstructures for this sample were given earlier [20].

2.2. 3D Microstructure within a Denticle

3D tissue observation of the claw denticles was performed in order to clarify how its tissue structure differed from those of the other two mineralized layers, as reported earlier [24]. Here, the denticle of the fixed finger shown in Figure 1c was observed. The serial-sectioning method using a Xe plasma type focused ion beam (PFIB)–SEM (Thermo Fisher Scientific Helios PFIB G4 UX, Waltham, MA, USA) was applied for 3D-reconstructed

image observation. The accelerating voltage of 2 kV was chosen to ensure a narrow slice pitch of 15 nm. Images were taken with a retractable type of annular back-scattered electron detector (BSE) placed just around an objective lens. Serial-sectioning observations were carried out along the z -direction, as described in later figure (Figure 2), and x - y plane images with every 15 nm pitch were observed for the surface and a position of $x = 1$ mm from the surface within the denticle. The 3D images were reconstructed using Image-Pro Premier 3D v9.2, Media Cybernetics visualization software (Rockville, MD, USA) from serial-sectioning images in the x - y plane obtained using a PFIB–SEM instrument.

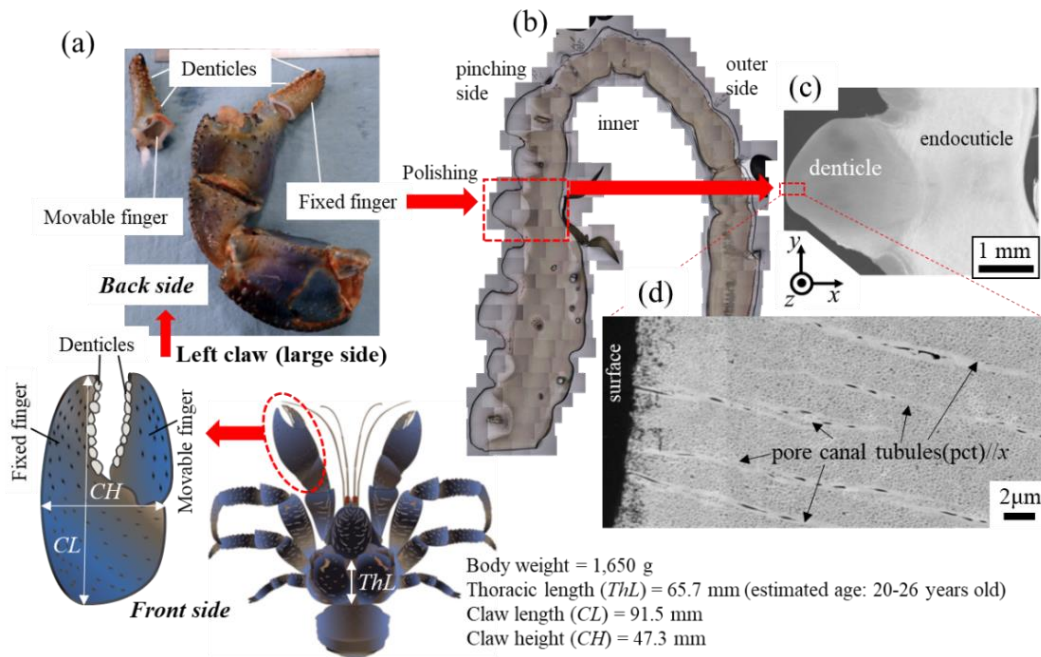


Figure 1. (a) Photographs of the left claw of the coconut crab used in the present study. Here, the movable finger was broken from the claw through the joint, and the fixed finger was cut by a saw. (b) Optical micrographs of a cross section of the fixed finger after polishing [20]. (c) Scanning electron microscope (SEM) image of the exoskeleton with the denticle on the pinching side and (d) a high-magnification SEM image of the denticle top.

2.3. Fracture Surface Observation

A fracture surface was observed in order to reveal the microstructures of the denticles. The test piece for observing the fracture surface was cut from the movable finger with a saw, and then the piece was placed in air for more than 48 h. A denticle in the test piece was broken by pinching with pliers. The surface of the fracture was coated with about 2 nm of osmium in order to obtain a clear microstructure image of organisms by eliminating the electron charge-up. The fracture surface was observed by SEM (JEOL JSM-7900F, Tokyo, Japan; accelerating voltage: 2 kV; detector: Everhart–Thornley type secondary electron detector (ET–SE)).

2.4. Observation from the Denticle Top

The top of some denticles was observed by SEM in order to examine macroscopically the existence of the epicuticle or exocuticle layer covering the denticle. The movable finger was cut with a saw. The piece was placed in air for more than 48 h before SEM observation and was coated with about 2 nm throughout the piece, including the denticle surface, as described in later figure (Figure 5a). The structural and chemical analyses were characterized using FIB–SEM (Thermo Fisher Scientific Scios 2, Waltham, MA, USA; accelerating voltage: 5 kV and 2 kV; detector: ET–SE) with energy-dispersive X-ray spectroscopy (EDS)

and a large silicon-drift detector (Oxford Instruments Ultim Max 170 EDS, Abingdon, Oxfordshire, GB).

3. Results and Discussion

3.1. 3D Microstructure

Figure 2 shows 3D microstructures at the surface and $x = 1$ mm from the surface within the denticle. The 3D animation corresponding to these microstructures can be seen in Videos S1 and S2 in the supporting information. Here, Figure 2a,c shows 3D images reconstructed with software without any special image processing, and Figure 2b,d shows 3D images reconstructed by coloring the edges of the high-brightness part with gold using the software.

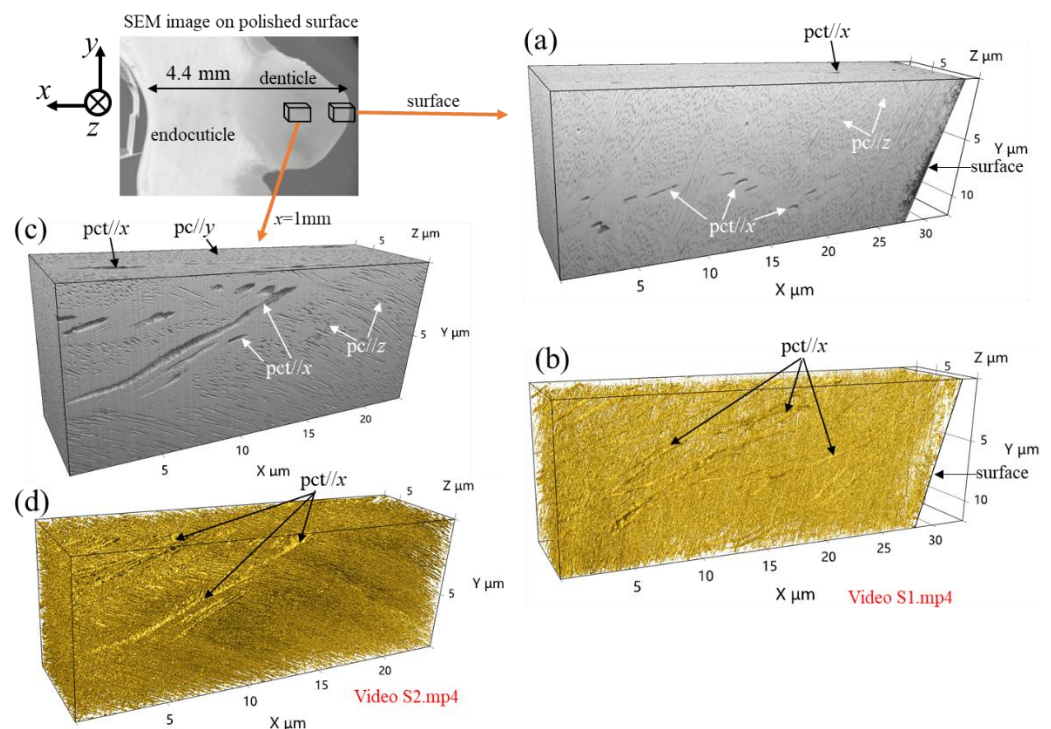


Figure 2. Three-dimensional (3D) microstructure in (a,b) surface and (c,d) $x = 1$ mm of the denticle. Each image was recorded with a slice pitch of 15 nm in the z -direction *via* a focused ion beam–SEM system, and 3D images were reconstructed using visualization software from serial-sectioning images in the x - y plane. (a,c) 3D images reconstructed through the software without any special image processing and (b,d) 3D images were reconstructed by coloring the edges of the high-brightness part with gold through the software.

In Figure 2a, the streaks extending in the x -direction observed on the x - y plane are traces of pore canal tubules (pct)// x , and they can be also seen on the x - z plane. Many black dots in the x - y and x - z planes are pore canals (pc), and the white color covering the whole represents mineralized substrate. The 3D image of the colored edges shown in Figure 2b and the corresponding 3D animations (Video S1) clearly demonstrate the presence of thick streaks (pct)// x extending in the x -direction and thin streaks (pct)// y and (pct)// z where those intersect. The microstructures in the x - y plane on the 3D image sliced by a FIB are the same as those of the SEM image of the polished surfaces, as shown in Figure 1d. These features can be visible in the 3D images $x=1$ mm from the surface, as shown in Figure 2c,d. The 3D results shown in Figure 2 and Videos S1 and S2 are different from those of the exocuticle (twisted plywood pattern structure) and endocuticle (porous structure) analyzed using the same method as reported earlier [24]. That is, the microstructure of the denticles is different than that of the two cuticle layers that have been revealed so far.

3.2. Fracture Surface

Figure 3 shows SEM micrographs of a fracture surface in the denticle. Note that the denticle observed is different from that shown in Figure 2. The denticle mainly has a tissue structure normal to the surface (Figure 3a), and the microstructure consists of a columnar-like pattern, as shown in Figure 3b,c. Its thickness was approximately 7–11 μm . This columnar-like structure can be observed extensively inside the denticle; surprisingly, the SEM image looks like a columnar joint belt formed as a result of lava flowing into the sea and rapidly cooling. The SEM images at the other two sites inside the denticle are shown in Figure S2 in the supplementary information, including the columnar joint belt which is the geological structure with the regular array of polygonal columns in Jeju Island of South Korea taken by one of the authors. The microstructure of the denticle seems to be a columnar joint belt. Hereafter, we refer to this structure as a columnar structure. The tissues normal to the surface shown in Figures 1d and 2 represent SEM images of the columnar structure on the polished surface and the surface sliced by FIB, respectively. On the other hand, on the denticle surface (Figure 3a), a layer with a tissue structure parallel to the surface, which is significantly different from the columnar structure, was observed, as shown in Figure 3d–f. The layer covering the columnar structure looks like a twisted plywood pattern structure rotated 180° around an axis normal to the surface, which is characteristic of the cuticle of crustaceans [11–14,17,24]. The stacking height, Sh , was 1.4 μm in Figure 3f, but the Sh decreased as it approached the surface. Furthermore, the epicuticle layer was observed in the outermost layer of the denticle. Namely, the denticle we observed on the fracture surface was covered by the epicuticle and exocuticle.

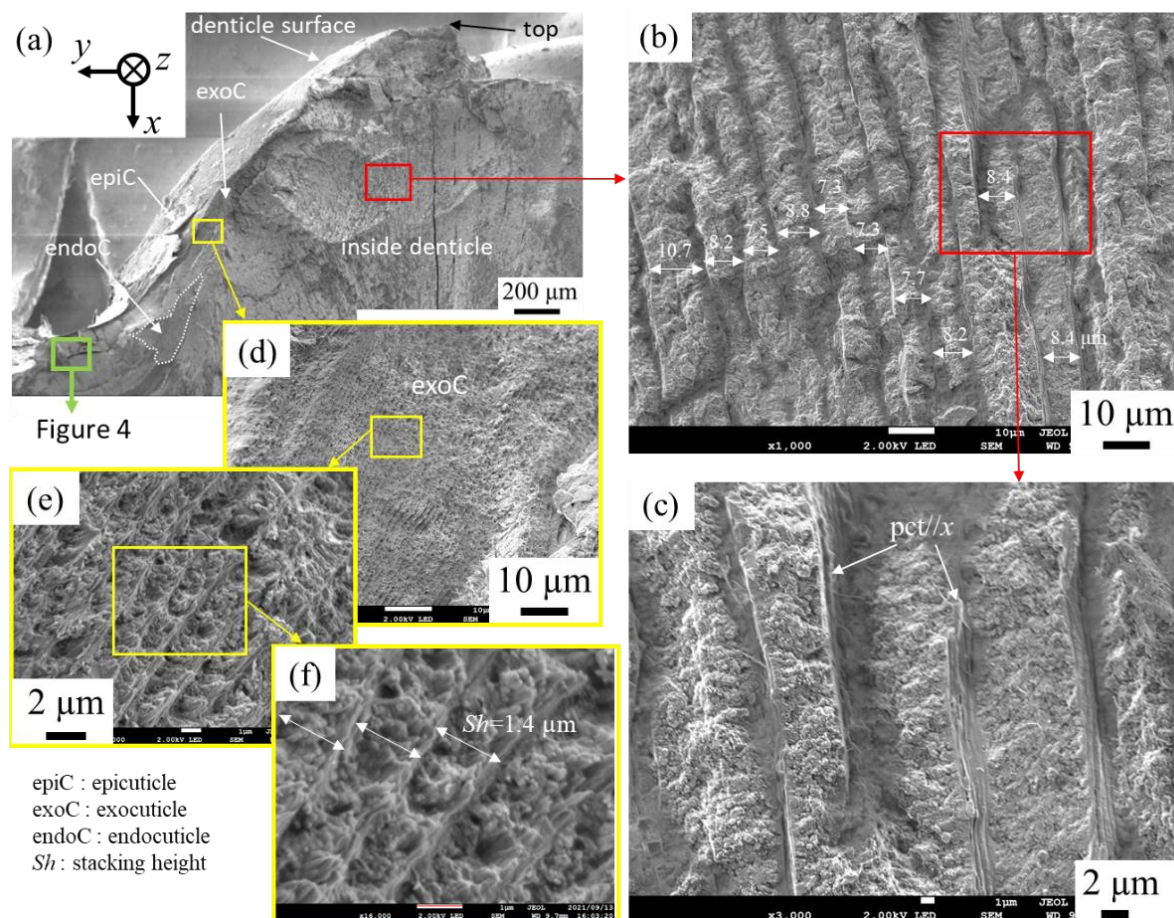


Figure 3. SEM micrograph of (a) a fracture surface of the denticle. Enlarged SEM micrographs of the area enclosed by rectangles in (a); (b,c) inside the denticle and (d–f) the exocuticle layer. Here, pct denotes pore canal tubules.

Next, the microstructures of the area surrounded by green in Figure 3a, corresponding to a valley part on the pinching side, were observed in detail. Figure 4 shows SEM micrographs at the area and enlarged micrographs of two different microstructures. In the layer near the surface (Figure 4b), a terrace-step fracture surface was observed in the region surrounded by dashed white line, and the layer consists of a twisted plywood structure as shown in Figure 4c. Such a fracture surface provides mechanical resistance to avoid catastrophic failure [25–29]. The terrace-step fracture surface has been often observed in the exocuticle layer on the fracture surface of coconut crab claws [15,25]. The fracture surface changes greatly with the intermediate layer as the boundary, as shown in Figure 4b, and the microstructure consists of a porous structure in which the pc//z is regularly arranged, as shown in Figure 4d. The spacing of the regularly arranged pc was $1.9\ \mu\text{m}$, as shown in Figure 4e. This porous structure seen in the endocuticle layer of the coconut crab was also visible in the region surrounded by a dashed white line in Figure 3a. That is, the valley part on the pinching side is composed of exocuticle, intermediate, and endocuticle, as observed on the outer side of the crab claws.

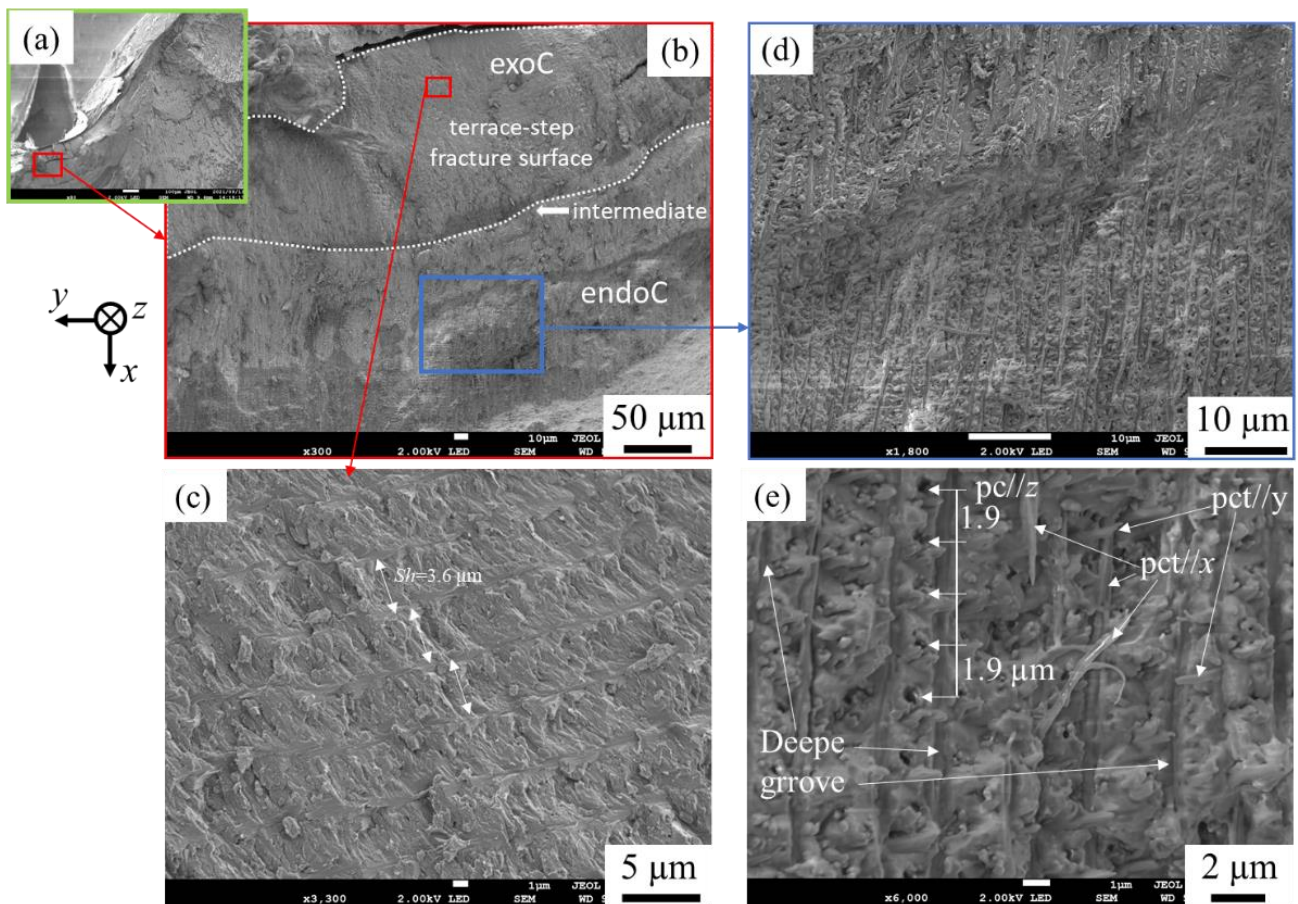


Figure 4. SEM micrograph near the valley of the (a) fracture surface of the denticle; (b) enlarged SEM micrographs of the area enclosed by rectangles in (a); SEM micrographs of (c,d) the endocuticle layer; and (e) the exocuticle layer. Here, pc denotes pore canal, and pct denotes pore canal tubules.

On the other hand, the tissue structure near the top of the denticle is unknown. Although there was no epi- or exocuticle near the denticle top, as shown in Figure 3a, these layers may have been lost when the denticle in the test piece was broken by pinching with pliers.

3.3. Denticle Surface

The results characterized by using a SEM from the denticle top are shown in Figure 5. One denticle in the specimen was missing and three denticles were seen (Figure 5a). Interestingly, in all three denticles, the thin layer (epi- or exocuticle) was lost only near the apex. The region of the columnar structure surface was indicated by a white dotted line in Figure 5b,c. Although it is difficult to clearly determine the region of the columnar structure surface on the denticles because the epicuticle and exocuticle layers are so thin, the judgment was based on the calcium (Ca) concentrations as determined by the point EDS analysis, as shown in Figure S3 in the supporting information, and the observation results *via* SEM. Here, in the case of a sample with large irregularities, as shown in Figure 5b,c, since it is very difficult to obtain the EDX map accurately and quantitatively due to the influence of shadowing and the problem of low statistical accuracy, a quantitative analysis of chemical compositions by the point measurements was performed. Denticle and exocuticle Ca concentrations, respectively, were in the range of 24 and 33 wt%, as reported earlier [15,20,24]. Since epicuticle is a non-mineralized substrate, the amount of Ca in the region covered with epicuticle is lower than that in the region without epicuticle. Note that EDS analysis also detects information regarding the thickness direction of several microns; therefore, the Ca concentration does not become zero even in the epicuticle region. Enlarged micrographs near the apex reveal the existence of thick *pc//x* and thin *pct* intersecting them (Figure 5d,e). Many pores related to *pct//x* were observed on the columnar structure surface. In addition, fibers were observed that were finer and denser than these of the pore canals on the surface (Figure 5f). These are thought to be chitin nanofibrils [30,31]. In denticle 2, crack marks during drying were observed on the surface (Figure 5g,h). The morphology of these characteristic cracks looks like the top of the columnar structure covering with the thin layers.

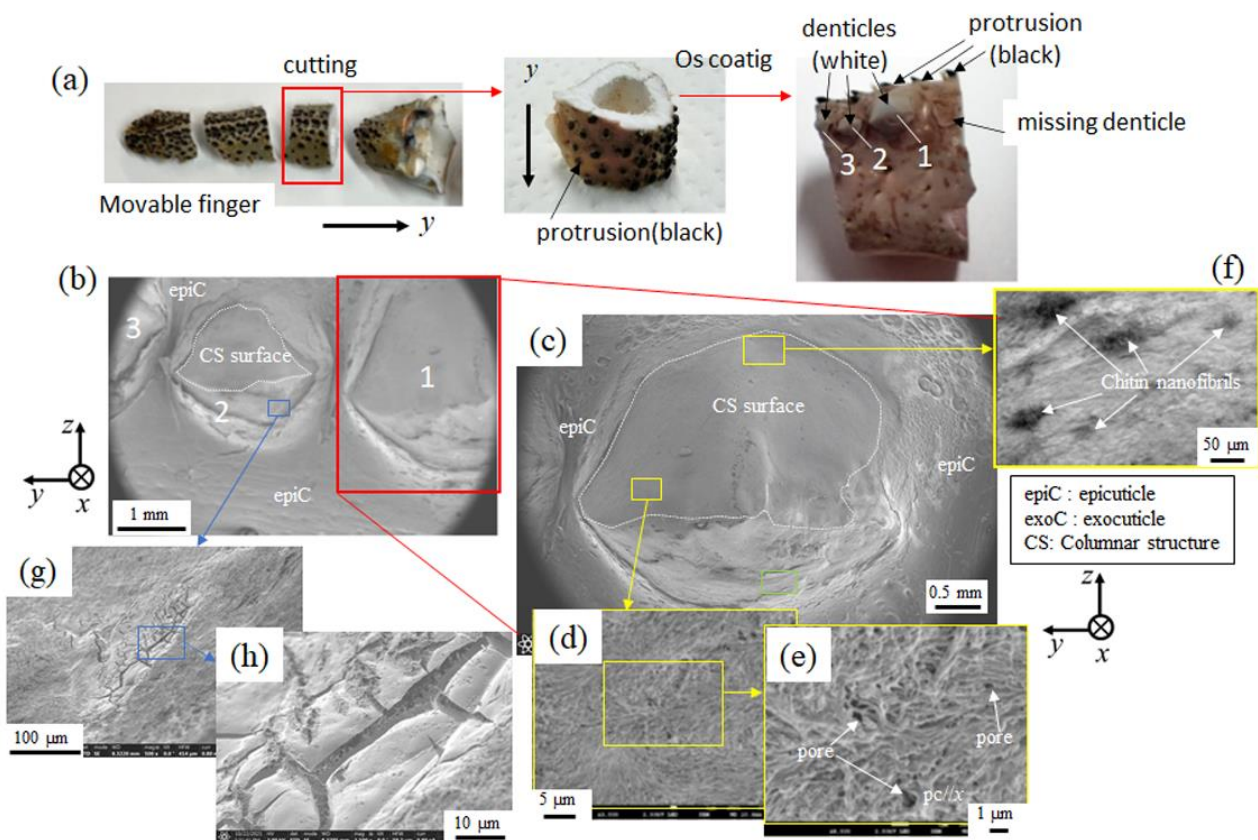


Figure 5. (a) Appearance of a sample after osmium coating and (b,c) SEM micrograph of the surface observed from the denticle top; (d–f) enlarged SEM micrographs of the area enclosed by yellow rectangles in (c); (g,h) enlarged SEM micrographs of the area enclosed by the blue rectangle in (b).

The denticles, which exist only on the pinching side of the claw, come into direct contact with predators and prey, and a large force is applied to them locally when pinched. In particular, the force is concentrated at the top of the denticle. Hence, the exocuticle, and certainly the epicuticle near the top of many denticles, should be lost due to abrasion. The coconut crab in the present study weighed 1650 g; Figure 6 shows SEM images of the denticle surfaces of claws of three coconut crabs weighing 1070 g, 610 g, and 300 g, which had been observed previously. The epicuticle and exocuticle were present on the columnar structure of the denticle in the 1070 g coconut crab (Figure 6a), and in the 610 g coconut crab, only the exocuticle was observed on the denticle surface (Figure 6b). However, these two layers were not found on the denticle surface of the 300 g coconut crab (Figure 6c). This is consistent with the result shown in Figures 1d and 2. The differences in these results appear to be related to the denticles and positions we observed rather than the size of the coconut crab.

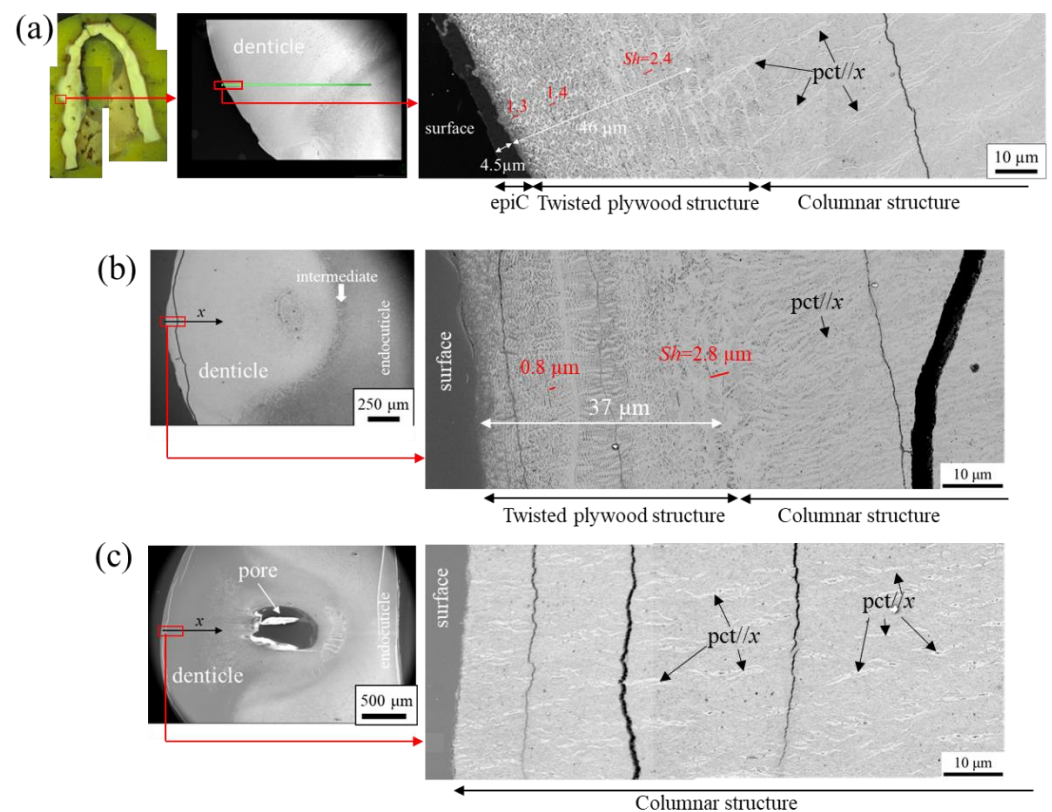


Figure 6. SEM micrographs of the denticle surface on the pinching side of the fixed finger of the left claw in coconut crabs of different sizes: (a) 1070 g, (b) 610 g, and (c) 300 g. Here, Sh denotes the stacking height of the twisted plywood structure, and pct denotes pore canal tubules.

Figure 7 shows the results from observing the surface of the pinching side of the fixed finger shown in Figure 1b with OM and SEM. The very thin and soft epicuticle layer may peel off and disappear during polishing, but the mineralized exocuticle layer does not. As shown by the red line in Figure 7b, the exocuticle layer was lost in the wide area above the large denticles; conversely, it could be observed in the surface of the relatively small denticles and in the base (i.e., the valley) of the denticle. The SEM micrograph of the denticle surface without the thin layers shown in Figure 7c agrees with that shown in Figures 1d and 6c. In Figure 7d, a lamellar structure (the exocuticle layer) parallel to the surface is visible on the denticle surface, and this structure disappears with the white arrow. The lamella spacing corresponds to the Sh , and the Sh becomes thicker from the outermost surface to the inside. That means that the exocuticle disappears with this white arrow due to abrasion. In other denticles, the high-magnification SEM micrograph (Figure 7e,f) at

the position where the exocuticle disappeared on the denticle surface revealed that there is a twisted plywood structure on the columnar structure and that the plywood structure disappears at the white arrow. According to the observation results so far [15,20], the Sh decreased as it approached the surface, and was less than $1\ \mu\text{m}$ in the outermost layer. However, the Sh shown in Figure 7f was more than $1\ \mu\text{m}$. This results from the abrasion of a part of the exocuticle layer existing on the surface of this denticle. This feature also has been seen in claw denticles of *Callinectes sapidus* and *Scylla serrata* [18].

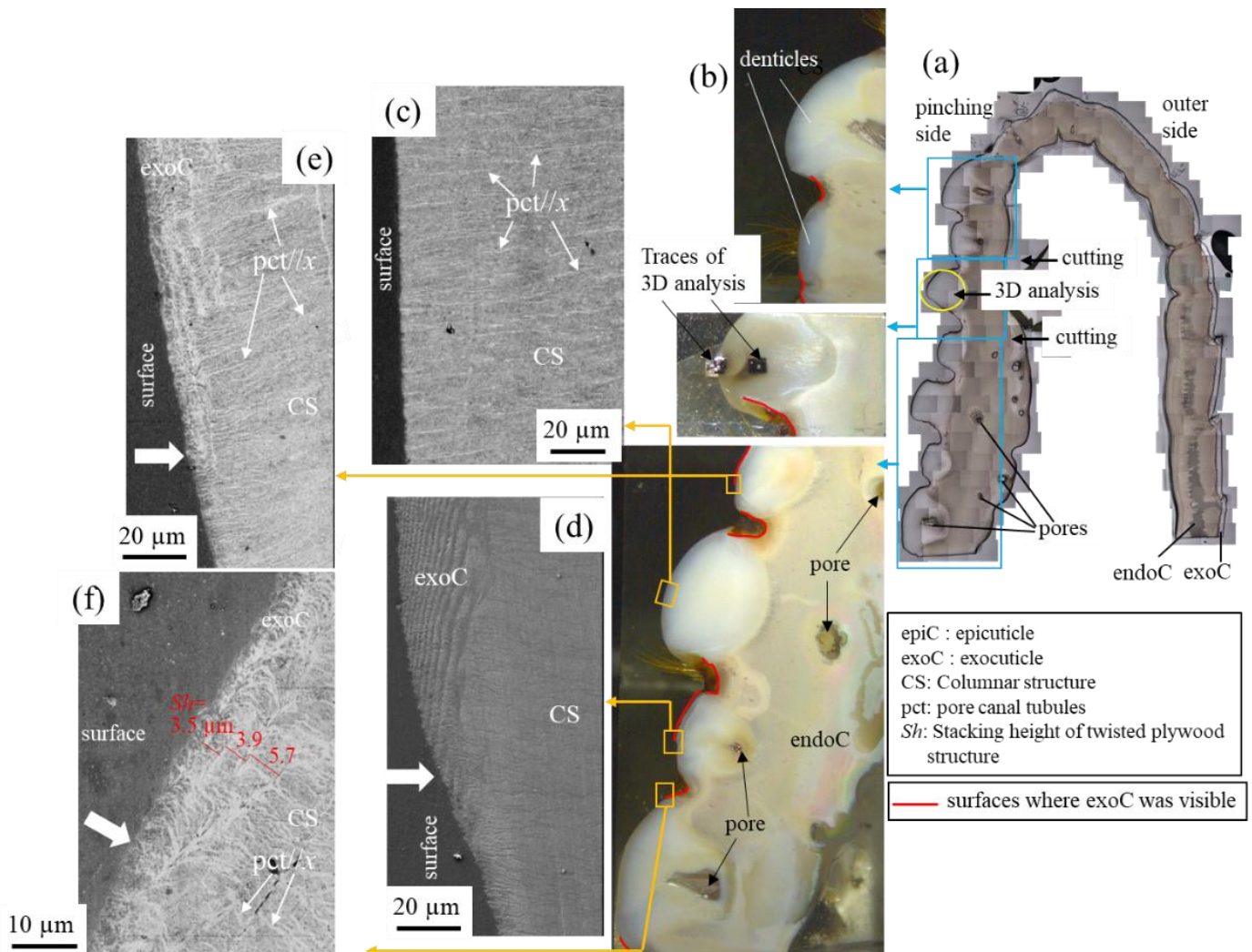


Figure 7. (a) Optical micrographs of a cross section of the fixed finger after polishing [20] and the cutting positions; (b) optical micrographs of the entire surface part of the pinching side. (c–f) SEM micrographs of the denticle surface with and without the exocuticle layer. Here, the white arrow denotes the position where the exocuticle disappeared on the denticle surface.

In short, as shown in Figure 1b and Figure S4 in the supplementary information, many large and small denticles irregularly exist on the pinching side of claws. Naturally, when pinching prey, the large denticle preferentially contacts the prey, and the contact area becomes large with increasing the pinching force. As a result, the opportunity for abrasion increases, and the epicuticle and exocuticle are lost. This indicates that the epicuticle and exocuticle do not play significant roles in the function of the denticle. In other words, denticles are thought to have been developed to make it easier to catch prey and food, as well as to make it easier to kill prey when pinched. In the exoskeleton that forms the denticle, there are spots where ions and nutrients are concentrated; columnar structures are formed through the spots, the exoskeleton is raised, and denticles covered with epicuticle

and exocuticle are formed. The existence of valleys is part of the process of denticle formation. The thin layers of the epicuticle and exocuticle are often lost due to abrasion. The irregular size of denticles makes it easier to catch prey and food of various types and shapes. Curiously, relatively large denticles are arranged in a line on the front side, and very small denticles are randomly arranged on the back side (Figure S4). This may be one of the characteristics of the omnivorous coconut crab's claws. The denticle microstructure was arranged normal to the surface, as shown in Figure 3. With this microstructure, cracks tend to progress inside, and the claws are more likely to be damaged. However, the intermediate layer between the denticle and the endocuticle is as soft [20], so only the denticles are thought to be damaged or lost before the claws are fractured. If some denticles are damaged or lost, the other denticles maintain the function of the claws, then molt, and new denticles develop. The various sizes, shapes, and irregularities of the denticles maximize the function of the claws. The columnar structure normal to the surface in the denticles may indicate a biomineralization that grows faster to form a convex shape in the exoskeleton, rather than a bioinspired structure that exhibits superior mechanical properties. We plan to examine these characteristics by comparing with other crustaceans denticles, and furthermore, the adaptive value of claw denticle would be revealed through stress analysis by a finite element simulation. Finally, we aim to develop bio-inspired materials by understanding the role of denticles, tissue structure, mechanical properties, and shape of claws, and using additive manufacturing.

The mineralized exoskeleton of the coconut crab's claw is classified into three structures: a twisted plywood pattern structure stacked parallel to the surface for the exocuticle, a porous structure with many regularly arranged pores vertical to the surface for the endocuticle [15,24], and a columnar structure vertical to the surface for the denticle. The denticles, which exist only on the pinching side of the claw, consist mainly of columnar structures and are covered with very thin epicuticles and exocuticles with a twisted plywood pattern structure. However, since the surface of the denticles comes into direct contact with predators and prey, the epicuticle and exocuticle layers are often lost due to abrasion, as shown in Figures 5 and 7. The presence of the thin layers on the outermost surface of the denticles is associated with the observed denticles and positions. The apex of the denticles and large denticles lose thinner layers because they have more opportunities for contact.

Supplementary Materials: The following supporting information can be downloaded at: <https://www.mdpi.com/article/10.3390/min12020274/s1>, Figure S1: X-ray diffraction (XRD) patterns of the denticle, exocuticle and endocuticle of the claw of male coconut crab (body weight: 610 g, thoracic length: 44.5 mm), including the standard x-ray diffraction of the calcite crystal, wako (FUJIFILM Wako Pure Chemical Co.). Here, XRD analysis at two positions for each layer was performed using commercial X-ray diffractometer SmartLab (Rigaku Co. Ltd., Tokyo, Japan). Figure S2: SEM micrograph of (a) a fracture surface of the denticle. (b,c) Enlarged SEM micrographs of the area enclosed by rectangles in (a). (d) A columnar joint belt on a Jeju Island, photographed in 2007 by one in the authors, T. Inoue. Figure S3: SEM micrograph of the denticle surface shown in Figure 5c and the point spectrum at some sites measured by energy-dispersive X-ray spectroscopy (EDS). Figure S4: Heterogeneous/irregular denticles (white) of the left claw's fixed finger of the coconut crab of male (body weight: 1150 g, thoracic length: 52.7 mm).

Author Contributions: Conceptualization, T.I.; methodology, T.I.; investigation, T.I.; resources, S.-i.O. and K.N.; data curation, T.I. and K.N.; writing—original draft preparation, T.I.; writing—review and editing, T.I., S.-i.O. and T.H.; visualization, T.I.; project administration, T.I.; funding acquisition, T.I. All authors have read and agreed to the published version of the manuscript.

Funding: This study was supported by JSPS KAKENHI Grant Number JP21H04537, Japan; the Uehara Memorial Foundation, Japan; Iketani Science and Technology Foundation (Grant No. 0331136-A), Japan. The grants are greatly appreciated.

Data Availability Statement: Not applicable.

Acknowledgments: We thank T. Hiroto, Y. Hara and Y. Kashihara for their experimental assistance with the microstructural observations and illustrations.

Conflicts of Interest: The authors declare no conflict of interest.

References

1. Islam, M.K.; Hazell, P.J.; Escobedo, J.P.; Wang, H. Biomimetic armour design strategies for additive manufacturing: A review. *Mater. Design* **2021**, *205*, 109730. [CrossRef]
2. Vincent, J.F. Survival of the cheapest. *Mater. Today* **2002**, *5–12*, 28–41. [CrossRef]
3. Wu, K.; Song, Z.; Zhang, S.; Ni, Y.; Cai, S.; Gong, X.; He, L.; Yu, S. Discontinuous fibrous Bouligand architecture enabling formidable fracture resistance with crack orientation insensitivity. *Proc. Natl. Acad. Sci. USA* **2020**, *117*, 15465–15472. [CrossRef] [PubMed]
4. Pan, L.; Wang, F.; Cheng, Y.; Leow, W.R.; Zhang, Y.W.; Wang, M.; Cai, P.; Ji, B.; Li, D.; Chen, X. A supertough electro-tendon based on spider silk composites. *Nature Commun.* **2020**, *11*, 1332. [CrossRef]
5. Yao, H.; Zheng, G.; Li, W.; McDowell, M.T.; Seh, Z.; Liu, N.; Lu, Z.; Cui, Y. Crab shells as sustainable templates from nature for nanostructured battery electrodes. *Nano Lett.* **2013**, *13*, 3385–3390. [CrossRef]
6. Cheng, L.; Thomas, A.; Glancey, J.L.; Karlsson, A.M. Mechanical behavior of bio-inspired laminated composites. *Compos. Part A* **2011**, *42*, 211–220. [CrossRef]
7. Launey, M.E.; Ritchie, R.O. On the fracture toughness of advanced materials. *Adv. Mater.* **2009**, *21*, 2103–2110. [CrossRef]
8. Locke, M. Pore canals and related structures in insect cuticle. *J. Biophys. Biochem. Cytol.* **1961**, *10*, 589–618. Available online: <https://www.jstor.org/stable/1603774> (accessed on 29 July 2020). [CrossRef] [PubMed]
9. Yano, I.; Kobayashi, S. Calcification and age determination in crustacea—I. Possibility of age determination in crabs on the basis of number of lamella in cuticles. *Bull. Jpn. Soc. Sci. Fish.* **1969**, *35*, 34–42. Available online: https://www.jstage.jst.go.jp/article/suisan1932/35/1/35_1_34/_pdf (accessed on 29 July 2020). [CrossRef]
10. Vittori, M.; Srot, V.; Korat, L.; Rejec, M.; Sedmak, P.; Bussmann, B.; Predel, F.; Aken, P.A.; Štrus, J. The Mechanical Consequences of the Interplay of Mineral Distribution and Organic Matrix Orientation in the Claws of the Sea Slater *Ligia pallasii*. *Minerals* **2021**, *11*, 1373. [CrossRef]
11. Bouligand, Y. Twisted fibrous arrangements in biological materials and cholesteric mesophases. *Tissue Cell* **1972**, *4*, 189–217. [CrossRef]
12. Raabe, D.; Sachs, C.; Romano, P. The crustacean exoskeleton as an example of a structurally and mechanically graded biological nanocomposite material. *Acta Mater.* **2005**, *53*, 4281–4292. [CrossRef]
13. Fabritius, H.-O.; Sachs, C.; Triguero, P.R.; Raabe, D. Influence of structural principles on the mechanics of a biological fiber-based composite material with hierarchical organization: The exoskeleton of the lobster *homarus americanus*. *Adv. Mater.* **2009**, *21*, 391–400. [CrossRef]
14. Sun, Y.; Tian, W.; Zhang, T.; Chen, P.; Li, M. Strength and toughness enhancement in 3d printing via bioinspired tool path. *Mater. Design* **2020**, *185*, 108239. [CrossRef]
15. Inoue, T.; Hara, T.; Nakazato, K.; Oka, S. Superior mechanical resistance in the exoskeleton of the coconut crab, *Birgus latro*. *Mater. Today Bio* **2021**, *12*, 100132. [CrossRef] [PubMed]
16. Boßelmann, F.; Romano, P.; Fabritius, H.; Raabe, D.; Epple, M. The composition of the exoskeleton of two crustacea: The American lobster *Homarus americanus* and the edible crab *Cancer pagurus*. *Thermochim. Acta* **2007**, *463*, 65–68. [CrossRef]
17. Chen, P.-Y.; Lin, A.Y.; McKittrick, J.; Meyers, M.A. Structure and mechanical properties of crab exoskeletons. *Acta Biomater.* **2008**, *4*, 587–596. [CrossRef] [PubMed]
18. Waugh, D.A.; Feldmann, R.M.; Schroeder, A.M.; Mutel, M.H. Differential cuticle architecture and its preservation in fossil and extant *Callinectes* and *Scylla* claws. *J. Crustacean Biol.* **2006**, *26*, 271–282. [CrossRef]
19. Rosen, M.N.; Baran, K.A.; Sison, J.N.; Steffel, B.V.; Long, W.C.; Foy, R.J.; Smith, K.E.; Aronson, R.B.; Dickinson, G.H. Mechanical resistance in decapod claw denticles: Contribution of structure and composition. *Acta Biomater.* **2020**, *110*, 196–207. [CrossRef] [PubMed]
20. Inoue, T.; Oka, S.; Nakazato, K.; Hara, T. Structural changes and mechanical resistance of claws and denticles in coconut crabs of different sizes. *Biology* **2021**, *10*, 1304. [CrossRef] [PubMed]
21. Drew, M.M.; Harzsch, S.; Stensmyr, M.; Erland, S.; Hansson, B.S. A review of the biology and ecology of the Robber Crab, *Birgus latro* (Linnaeus, 1767) (Anomura: Coenobitidae). *Zool. Anz.* **2010**, *249*, 45–67. [CrossRef]
22. Oka, S.; Tokutake, K.; Inoue, T. Growth analysis and population size estimation of coconut crabs based on a large recapture dataset. *Crustacean Res.* **2021**, *50*, 145–150. [CrossRef]
23. Oka, S.; Matsuzaki, S.; Toda, M. Identification of individual coconut crabs, *Birgus latro*, on the basis of the pattern of grooves on the carapace. *Crustacean Research* **2013**, *42*, 17–23. [CrossRef]
24. Inoue, T.; Oka, S.; Hara, T. Three-dimensional microstructure of robust claw of coconut crab, one of the largest terrestrial crustaceans. *Mater. Design* **2021**, *206*, 109765. [CrossRef]
25. Inoue, T.; Kimura, Y.; Ochiai, S. Shape effect of ultrafine-grained structure on static fracture toughness in low-alloy steel. *Sci. Technol. Adv. Mater.* **2012**, *13*, 035005. [CrossRef]

26. Kakisawa, H.; Sumitomo, T. The toughening mechanism of nacre and structural materials inspired by nacre. *Sci. Technol. Adv. Mater.* **2011**, *12*, 064710. [[CrossRef](#)] [[PubMed](#)]
27. Inoue, T.; Yin, F.; Kimura, Y.; Tsuzaki, K.; Ochiai, S. Delamination effect on impact properties of ultrafine-grained low-carbon steel processed by warm caliber rolling. *Metall. Mater. Trans. A* **2010**, *41*, 341–355. [[CrossRef](#)]
28. Pozuelo, M.; Carreno, F.; Ruano, O.A. Delamination effect on the impact toughness of an ultrahigh carbon-mild steel laminate composite. *Compos. Sci. Technol.* **2006**, *66*, 2671–2676. [[CrossRef](#)]
29. Inoue, T.; Ueji, R. Improvement of strength, toughness and ductility in ultrafine-grained low-carbon steel processed by warm bi-axial rolling. *Mater. Sci. Eng. A* **2020**, *786*, 139415. [[CrossRef](#)]
30. Meyers, M.A.; Chen, P.Y.; Lin, A.Y.M.; Seki, Y. Biological materials: Structure and mechanical properties. *Prog. Mater. Sci.* **2008**, *53*, 1–206. [[CrossRef](#)]
31. Ifuku, S.; Nogi, M.; Abe, K.; Yoshioka, M.; Morimoto, M.; Saimoto, H.; Yano, H. Preparation of chitin nanofibers with a uniform width as α -chitin from crab shells. *Biomacromolecules* **2009**, *10*, 1584–1588. [[CrossRef](#)] [[PubMed](#)]